BIOCHIP JOURNAL, Vol. 3, No. 4, 275-280, December 2009

Hydrodynamically Focused Particle Filtration Using an Island Structure

Kangsun Lee[1], Choong Kim[2], Byungwook Ahn[1], Ji Yoon Kang[2] & Kwang W. Oh[1]

[1]SMALL (Sensors and MicroActuators Learning Lab), Department of Electrical Engineering, The State University of New York at Buffalo, Buffalo, NY 14260, USA
[2]Nano-Bioresearch Center, Korea Institute of Science and Technology (KIST), 39-1 Hawolgok Dong, Seongbuk Gu, Seoul 136-791, Korea
Correspondence and requests for materials should be addressed to K.W. Oh (kwangoh@buffalo.edu)

Accepted 24 September 2009

Abstract

We propose a particle filtration method based on hydrodynamic focusing. Three microchannels associated for the filtration were networked with an island structure to control a boundary to limit particle sizes. By adjusting the ratios of hydraulic resistances of the three microchannels, the boundary distance was controlled. Using hydrodynamic focusing in the microfluidic network, we have successfully designed and tested the device to filtrate particles of 10 μm and 20 μm. The proposed method can continuously separate particles by size. Thus, the proposed separation method can be applicable for many fields in biology and biomedical engineering.

Keywords: Hydrodynamic focusing, Particle filtration, Separation, Microfluidics

Introduction

Recently, the separation of microparticles, such as microbeads, microorganisms, and cells in complex samples, has been required for biochemical and biomedical analysis[1,2]. For instance, microbeads labeled with antibodies and ligands are separated for molecular recognition of proteins and DNA in biological systems[3,4]. Separation also plays an important role in the analysis of blood, stem, and tumor cells[5]. When performing blood analysis in medical laboratories, the blood cells are separated from whole blood by centrifugation. Then the purified blood plasma is analyzed for electrolyte concentration, glucose, lactate, total cholesterol, etc, or the concentrated blood cells (e.g., RBCs and WBCs) are quantified using flow cytometers.

Size-dependent separation or filtration is one of the promising technologies in biomedical engineering. Microparticles and cells have been separated by properties such as density[6], size[7-10], surface property[11,12], magnetism[13], dielectrophoretic characteristics[14,15], etc. Among these, we focus on size because it is one of the simplest particle properties and is widely applicable. Previous methods use micro/nanofabricated filters[16,17] or pinched flow fractionation near sidewalls[8,9]. However, these previous particle separators presented major problems, including particle adhesion or clogging to the sidewalls or the mechanical structures, and slow separation due to particle positioning near the sidewalls.

On the other hand, in this paper, particles are hydrodynamically focused and continuously separated in the middle of a microchannel, where the flow velocity is the highest and an island structure is embedded to align and separate the particles. The positioning of the particles in the middle rather than near the sidewalls has many advantages: no particle adhesion or clogging to the sidewall, high-speed separation due to a high flow velocity in the middle of the microchannel, and precise control of a boundary to separate particles by size due to easy control of the volumetric flow rates in the middle of the channel. In addition, the filtration of various particle sizes is possible because the boundary distance is easily adjustable by controlling the hydraulic channel resistances in a microfluidic network.

Principle

The principle of hydrodynamically focused particle filtration is shown in Figure 1. Microparticles are hydrodynamically focused to the center of a focusing channel by sheath flows injected from two side inlet channels. A laminar fluid flow containing the hydrodynamically focused particles is continuously introduced into a filtration zone in the left-to-right direction. In the center of the filtration zone, where the flow velocity is highest, an island structure is in place. There exists a boundary distance *d* from the island sidewalls that divides the laminar fluid flow into a main stream flowing into a main outlet channel A, and two side streams flowing into two side outlet channels B and C.

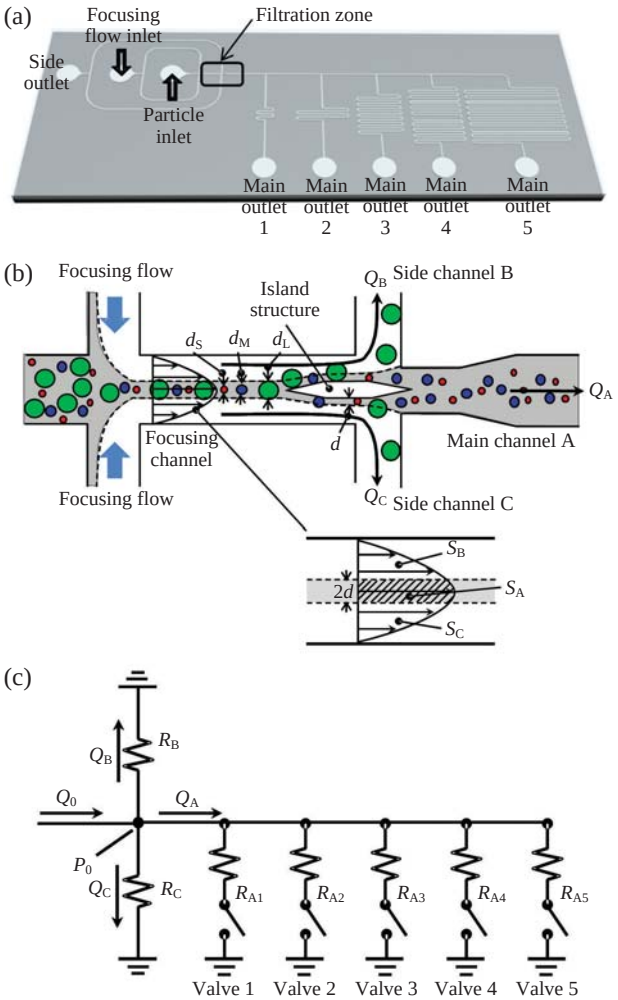

Figure 1. Schematic of continuous particle filtration using hydrodynamic focusing in a microfluidic network. (a) A layout of a device, (b) a filtration zone, and (c) an equivalent electric circuit.

A key idea to filter the particles by size is to control the boundary distance d by adjusting the ratio of volumetric flow rates, Q_A and Q_B ($=Q_C$). Q_A is the volumetric flow in the main outlet channel A, and Q_B and Q_C are the volumetric flows in the side outlet channels B and C. Figure 1c shows an equivalent electric circuit that represents the microfluidic circuit shown in Figure 1a. When the flow is pressure-driven and laminar, and the fluid is a non-compressive Newtonian fluid, the flow profile will be parabolic. The volumetric flow rate Q in a straight microchannel is represented as follows: $Q=\Delta P\times(1/R)$, where ΔP is the pressure loss between channel ends and R is the hydrodynamic resistance of the microchannel. Since all outlets are grounded, the pressure losses (ΔP_A, ΔP_B, and ΔP_C) through the channels A, B, and C are identical to $P_0 : \Delta P_A=\Delta P_B=\Delta P_C=P_0=Q_A\times R_A=Q_B\times R_B=Q_C\times R_C$. Therefore, the distribution of volumetric flow rates, which determines the size limit of the filtered particles, is easily determined by the ratio between hydraulic resistances, R_A and R_B ($=R_C$). If the cross-sections of all microchannels in the microfluidic circuit are identical, the hydraulic resistance is simply proportional to the channel length L[18-20].

Thus, the virtual width of the flow entering into the main channel A, $2d$, can be predicted from the ratio of hydraulic resistances, assuming that the flow profile is parabolic (Figure 1b). The partial area of the parabola is proportional to the volumetric flow rate; $S_A : S_B=Q_A : Q_B=1/R_A : 1/R_B=1/L_A : 1/L_B$. The hypothesis is that particles whose radius is smaller than the boundary distance d would follow the main stream into the main outlet channel A. Particles whose radius is larger than the boundary distance d would follow the side streams into two side outlet channels B and C. Considering three particles whose diameters are d_S, d_M, and d_L, as shown in Figure 1b, the boundary distance d can be expressed as follows: $d_S/2<d_M/2<d<d_L/2$. In this concept, the filtration of various particle sizes is possible because the boundary distance is easily adjustable using built-in valves that control the hydraulic channel resistances in a microfluidic network.

Results and Discussion

Device Characterization

First, the device was characterized by varying the hydraulic resistance ratios by closing/opening each valve. When the valves 1, 2, 3, 4, and 5 were open, $R_A=R_B$, $R_A=2\ R_B$, $R_A=4\ R_B$, $R_A=8\ R_B$, and $R_A=16\ R_B$, respectively. When the valve 1 was open, the ratio between hydraulic resistances, R_A and R_B ($=R_C$), was unit; that is, $Q_A=Q_B$ or $S_A=S_B$. At this state, the 10-μm particles (Figure 2a) and the 20-μm particles (Figure 2b) flew into the main channel A. On the other hand, when the valve 4 was open, the 10-μm particles flew into the main channel A (Figure 3a), but the 20-μm particles moved out into the side channels (Figure 3b).

Filtration Efficiency

We measured the filtration efficiencies as a function of the ratios between L_A and L_B by opening/closing each valve. Figure 4 shows the summary of the performance of the device. When the valves 1 and 2 were open, all of the particles moved into the main channel A. The boundary distance d must be larger than the radius of the particles ($d>\sim10$ μm). When the valve 3

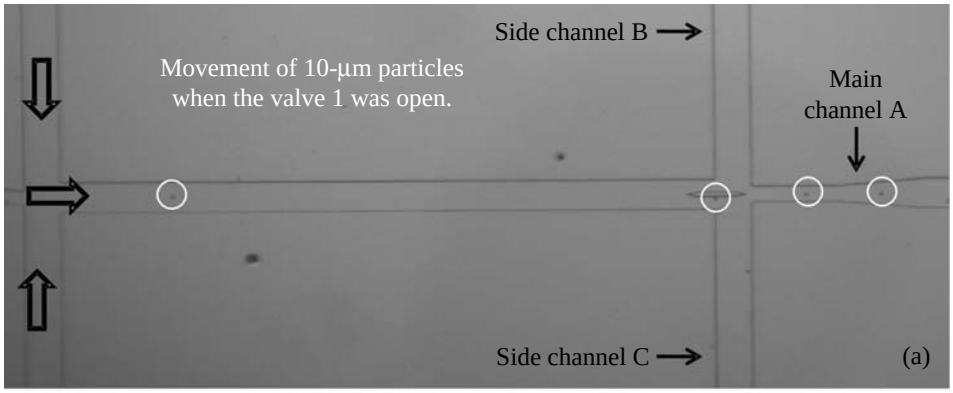

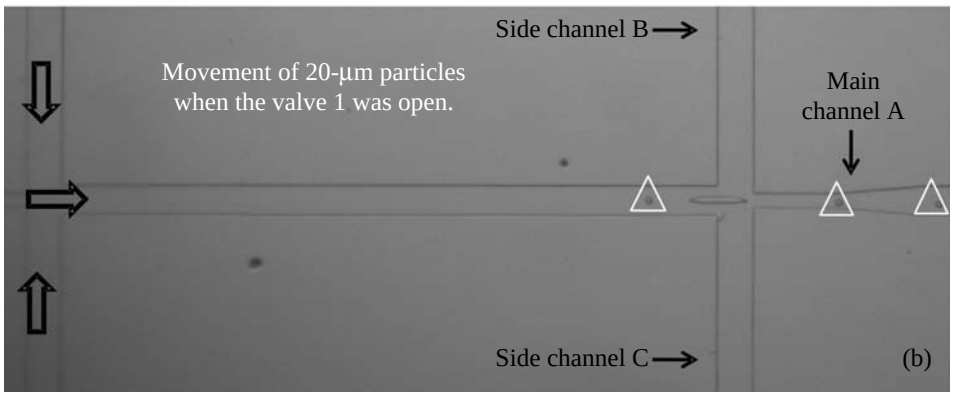

Figure 2. When $R_A = R_B$ (the valve 1 was open), all of particles (10-μm and 20-μm particles) flew into the main channel due to $d > \sim 10$ μm. Images of the sorting zone for (a) the 10-μm particles and (b) the 20-μm particles. Circles for the 10-μm particles and triangles for the 20-μm particles.

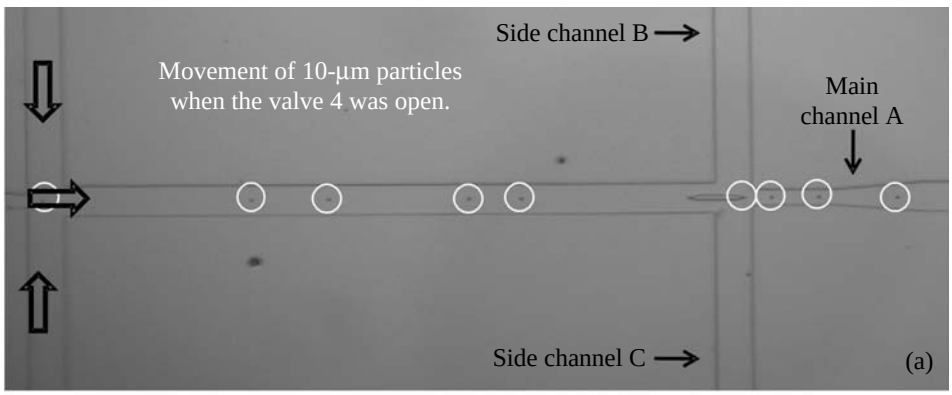

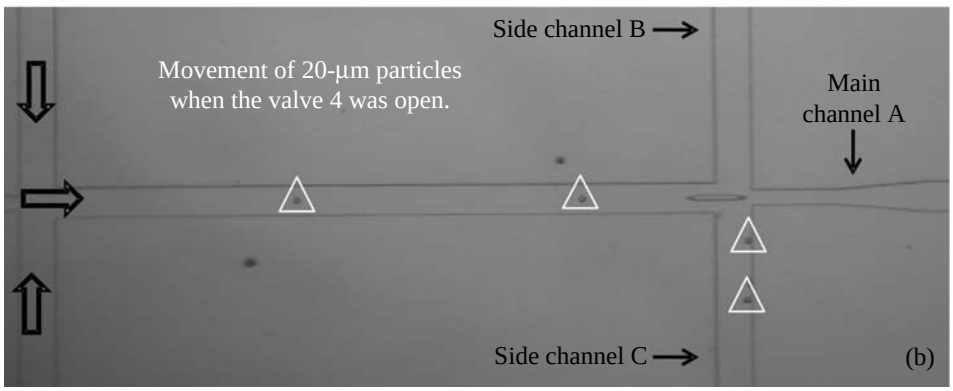

Figure 3. When $R_A = 8\ R_B$ (the valve 4 was open), 10-μm particles flew into the main channel and 20-μm particles moved out into the side channels due to $d < \sim 10$-μm. Images of the sorting zone for (a) the 10-μm particles and (b) the 20-μm particles. Circles for the 10-μm particles and triangles for the 20-μm particles.

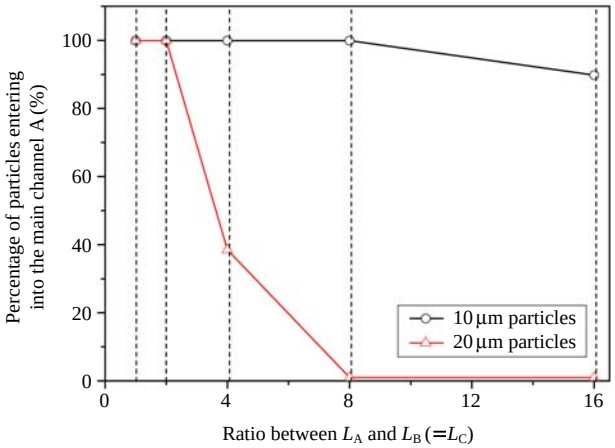

Figure 4. Filtration efficiencies as a function of ratios between L_A and L_B. When the valves 1, 2, 3, 4, and 5 were open, R_A=R_B, R_A=2 R_B, R_A=4 R_B, R_A=8 R_B, and R_A=16 R_B, respectively.

was open (R_A=4 R_B, Q_A=1/4 Q_B or S_A=1/4 S_B), ~40% of the 20-μm particles showed up in the main outlet 3 (d=~10 μm). When the valve 4 was open (R_A=8 R_B, Q_A=1/8 Q_B or S_A=1/8 S_B), no 20-μm particles entered into the main channel. At this state, the boundary distance d must be larger than the radius of the 10-μm particles and smaller than the radius of the 20-μm particles (~5 μm < d < ~10 μm). When the valve 5 was open, ~10% of the 10-μm particles moved out into the side channels; the boundary distance d is expected to be close to ~5 μm when R_A=~16 R_B.

Filtration of Multiplexed Particles

We then performed the filtration experiment using a mixture of the 10-μm and the 20-μm particles. From the above-mentioned experiment, we determined the condition for the filtration of the mixture. When R_A= 8 R_B, we could filter the 20-μm particles from the mixture due to ~5 μm < d < ~10 μm. Figure 5 shows the filtration experiment using the mixture of 10-μm and 20-μm particles when the valve 4 was open. The filtration efficiencies were 85.7% for the 20-μm particles in the side outlet and 97.5% for the 10-μm particles in the main outlet 4. In the main outlet 4, most of particles were 10-μm particles. The 20-μm particles were successfully filtered out from the mixture. Only 2.5% of the 20-μm particles showed up in the main outlet 4. Therefore, the proposed device is very efficient in the filtration of large particles from inhomogenous mixtures. For instance, by connecting filtration stages in series, multiplexed microparticles can be filtered in series. The largest particles can be filtered at the first stage. Then the second largest particles can

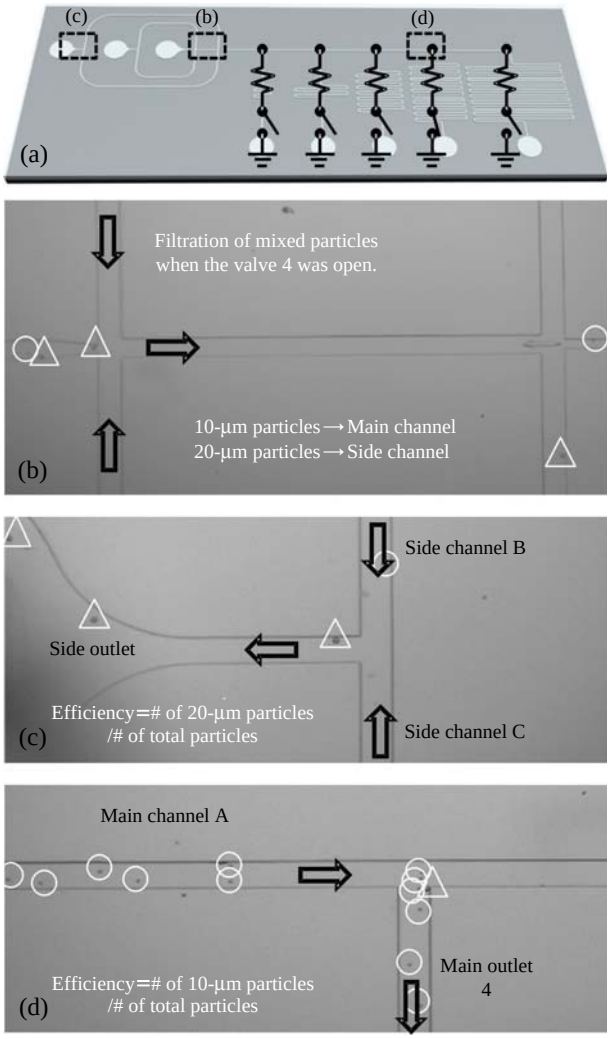

Figure 5. (a) Filtration experiment of a mixture of 10-μm and 20-μm particles when the valve 4 was open. Photo images of (b) the filtration zone, (c) the side outlet, and (d) the branch between the main channel A and the main outlet 4.

be filtered at the second stage, and so on. This multiplexed particle filtration device will be useful for whole blood filtration (e.g., WBCs, RBCs, and serum).

Conclusions

We have designed and tested the size-dependent filtration device using hydrodynamic focusing with the island structure embedded in the microfluidic network. By adjusting the ratios of the hydraulic resistances of three microchannels associated with the filtration, we were able to attain a high filtration efficiency of 97.5% for the 10-μm particles from a mixture of the 10-μm

and 20-μm particles. In addition, closing/opening each valve allowed easy control of the boundary distance from the island structure. Thus, the proposed method can be applicable for many fields, especially in filtration of particles in rough sizes such as blood cell separation and removal of cell clumps for single-cell collections.

Materials and Methods

Device Fabrication

A polydimethylsiloxane (PDMS) device was fabricated by conventional soft lithography. For a soft mold, negative photoresist (SU-8 2025) was spin-coated on a silicon wafer with a thickness of 50 μm, and patterned using a conventional UV photolithography method. Microfluidic channels and the island structure were molded. The widths of channels A, B, and C were 100 μm, and the neck of the main channel A was 50 μm. The width of the island structure was 20 μm. L_B and L_C (the lengths of channels B and C, respectively) were 17 mm, and L_{A1}, L_{A2}, L_{A3}, L_{A4}, and L_{A5} were 1×, 2×, 4×, 8×, and 16× (times) the L_B, respectively. A glass substrate and the molded PDMS layer were subsequently exposed to O^2 plasma, and sealed irreversibly. Then, we baked the device on a hotplate for 1 hr at 70˚C to increase bonding strength between the glass substrate and the PDMS layer.

Experimental Set up

As model particles, 10-μm and 20-μm single polystyrene microbeads (Cat. number 4210A and 4220A, Duke Scientific Corp., Palo Alto, CA) were used. The device was connected with silicon tubing with inner diameter of 0.5 mm. Then, the tubing connected with a polypropylene L-shaped connector was inserted into inlets and outlets. All solutions were injected by precise syringe pumps (KD scientific). The flow rates were 10 μL/hr for the particle flow (with a concentration of ~100 particles/μL) and 300 μL/hr for the focusing flow. Experimental results were captured by a Nikon stereo-type microscope. Each valve was closed by plugging a sealed cap into each main outlet port.

Acknowledgements

This research was supported in part by the Intelligent Microsystem Center, which is carrying out one of the 21st Century's Frontier R&D Projects sponsored by the Korea Ministry of Commerce, Industry and Energy.

References

1. Pappas, D. & Wang, K. Cellular separations: A review of new challenges in analytical chemistry. *Analytica Chimica Acta* **601**, 26-35 (2007).
2. Radisic, M. *et al.* Micro- and nanotechnology in cell separation. *Int. J. Nanomedicine*. **1**, 3-14 (2006).
3. Miwa, J. *et al.* Adhesion-based cell sorter with antibody-coated amino-functionalized-parylene surface. *J. Microelectromech. Syst.* **17**, 611-622 (2008).
4. Yun, K.S. *et al.* A microfluidic chip for measurement of biomolecules using a microbead-based quantum dot fluorescence assay. *Meas. Sci. Technol.* **17**, 3178-3183 (2006).
5. Adams, A.A. *et al.* Highly efficient circulating tumor cell isolation from whole blood and label-free enumeration using polymer-based microfluidics with an integrated conductivity sensor. *J. Am. Chem. Soc.* **130**, 8633-8641 (2008).
6. Carlo, D.D. *et al.* Continuous inertial focusing, ordering, and separation of particles in microchannels, *PNAS* **104**, 18892-18897 (2007).
7. Huang, L.R. *et al.* Continuous particle separation through deterministic lateral displacement. *Science* **304**, 987-990 (2004).
8. Takagi, J. *et al.* Continuous particle separation in a microchannel having asymmetrically arranged multiple branches. *Lab Chip* **5**, 778-784 (2005).
9. Yamada, M. & Seki, M. Hydrodynamic filtration for on-chip particle concentration and classification utilizing microfluidics. *Lab Chip* **5**, 1233-1239 (2005).
10. Bhagat, A.A.S. *et al.* Continuous particle separation in spiral microchannels using dean flows and differential migration. *Lab Chip* **8**, 1906-1914 (2008).
11. Dhayal, M. *et al.* Biological fluid interaction with controlled surface properties of organic micro-fluidic devices. *Vacuum* **80**, 876-879 (2006).
12. Chang, W.C. *et al.* Biomimetic technique for adhesion-based collection and separation of cells in a microfluidic channel. *Lab Chip* **5**, 64-73 (2005).
13. Han, K.H. & Frazier, A.B. Paramagnetic capture mode magnetophoretic microseparator for high efficiency blood cell separations. *Lab Chip* **6**, 265-273 (2006).
14. Hughes, M.P. Strategies for dielectrophoretic separation in laboratory-on-a-chip systems. *Electrophoresis* **23**, 2569-2582 (2002).
15. Park, J. *et al.* An efficient cell separation system using 3D-asymmetric microelectrodes. *Lab Chip* **5**, 1264-1270 (2005).
16. Choi, S. *et al.* Continuous blood cell separation by hydrophoretic filtration. *Lab Chip* **7**, 1532-1538 (2007).
17. Chen, X. *et al.* Microfluidic chip for blood cell separation and collection based on crossflow filtration. *Sens. Actuators*: *B* **130**, 216-221 (2008).
18. Lee, K. *et al.* Generalized serial dilution module for monotonic and arbitrary microfluidic gradient genera-

tors. *Lab Chip* **9**, 709-717 (2009).
19. Lee, K. *et al.* 2-Layer based microfluidic concentration generator by hybrid serial and volumetric dilutions. *Biomed Microdevices*, submitted (2009).
20. Lee, K. *et al.* Microfluidic network-based combinatorial dilution device for high throughput screening and optimization. *Microfluid. Nanofluid*., DOI 10.1007/s10404-009-0500-z (2009).